The EMBO Journal (2008) 27, 1231–1242 | © 2008 European Molecular Biology Organization | All Rights Reserved 0261-4189/08
www.embojournal.org

THE EMBO JOURNAL

A crucial role of WW45 in developing epithelial tissues in the mouse

Joo-Hyeon Lee[1], Tae-Shin Kim[1], Tae-Hong Yang[1], Bon-Kyoung Koo[2], Sang-Phil Oh[1], Kwang-Pyo Lee[1], Hyun-Jung Oh[1], Sang-Hee Lee[3], Young-Yun Kong[2], Jin-Man Kim[4] and Dae-Sik Lim[1,*]

[1]National Research Laboratory, Department of Biological Sciences, Korea Advanced Institute of Science and Technology, Daejeon, Korea, [2]Division of Molecular and Life Sciences, Pohang University of Science and Technology, Kyungbuk, Korea, [3]Division of Electron microscopic Research, Korea Basic Science Institute, Daejeon, Korea and [4]Department of Pathology, College of Medicine, Chungnam National University, Daejeon, Korea

The role and molecular mechanisms of a new Hippo signalling pathway are not fully understood in mammals. Here, we generated mice that lack WW45 and revealed a crucial role for WW45 in cell-cycle exit and epithelial terminal differentiation. Many organs in the mutant mouse embryos displayed hyperplasia accompanied by defects in terminal differentiation of epithelial progenitor cells owing to impaired proliferation arrest rather than intrinsic acceleration of proliferation during differentiation. Importantly, the MST1 signalling pathway is specifically activated in differentiating epithelial cells. Moreover, WW45 is required for MST1 activation and translocation to the nucleus for subsequent LATS1/2 activation upon differentiation signal. LATS1/2 phosphorylates YAP, which, in turn, translocates from the nucleus into the cytoplasm, resulting in cell-cycle exit and terminal differentiation of epithelial progenitor cells. Collectively, these data provide compelling evidence that WW45 is a key mediator of MST1 signalling in the coordinate coupling of proliferation arrest with terminal differentiation for proper epithelial tissue development in mammals.

The EMBO Journal (2008) **27,** 1231–1242. doi:10.1038/emboj.2008.63; Published online 27 March 2008
Subject Categories: signal transduction; differentiation & death
Keywords: epithelial proliferation and differentiation; hWW45; MST1 signalling

Introduction

Homeostasis of regenerative epithelial tissues such as skin and intestine is maintained through a tightly balanced process of proliferation and terminal differentiation. During normal epithelial development, proliferating progenitor cells, often referred to as transiently amplifying cells, actively divide a limited number of times before they undergo cell-cycle exit and terminally differentiate into postmitotic cells (Blanpain *et al*, 2007). Cancer can develop as a result of inappropriate proliferation of progenitor cells accompanied by a partial or complete loss of differentiation (Reya *et al*, 2001). Therefore, understanding the signalling networks that control cell-cycle exit and terminal differentiation in epithelial tissues will provide insights into the mechanisms underlying tumorigenesis.

A new signalling network, known as the 'Hippo pathway' in *Drosophila*, seems to be a key developmental programme in controlling proliferation and apoptosis for proper organ development in *Drosophila* (Edgar, 2006; Harvey and Tapon, 2007; Pan, 2007; Saucedo and Edgar, 2007). The Ste-20 family kinase Hippo (Harvey *et al*, 2003; Jia *et al*, 2003; Pantalacci *et al*, 2003; Udan *et al*, 2003; Wu *et al*, 2003), WW adaptor protein Salvador (Kango-Singh *et al*, 2002; Tapon *et al*, 2002) and NDR kinase Warts (Justice *et al*, 1995; Xu *et al*, 1995) are the key components of the Hippo pathway that restrict cell proliferation and promote apoptosis in differentiating epithelial cells by regulating expression of cyclin E and Diap1. The Hippo kinase phosphorylates and activates the Warts kinase, and this process is facilitated by the scaffolding protein Salvador or Mats (Wu *et al*, 2003; Wei *et al*, 2007). Warts, together with Mats, then phosphorylates and inhibits the transcription coactivator Yorkie (Huang *et al*, 2005; Lai *et al*, 2005). Expanded, Merlin and Fat, all of which localize to the plasma membrane, function upstream of the Hippo pathway (Bennett and Harvey, 2006; Cho *et al*, 2006; Hamaratoglu *et al*, 2006; Silva *et al*, 2006; Willecke *et al*, 2006). In flies, mutations of these factors lead to increased cell proliferation and decreased cell death.

The phenotypes of flies with mutations in the Hippo pathway can be rescued with their respective human counterparts (Tao *et al*, 1999; Wu *et al*, 2003; Huang *et al*, 2005; Lai *et al*, 2005), indicating that the Hippo pathway may have an analogous role in epithelial tissue development in mammals. Several reports on each mammalian component of the Hippo pathway have shown that the pathway is involved in cell death and cell-cycle regulation. MST1/2 kinases (Hippo homologues) were originally reported to be involved in apoptosis with caspase-3-mediated proteolytic activation (Lee *et al*, 1998). LATS1/2 (Warts homologues) have been implicated in the regulation of cell-cycle progression, apoptosis (Tao *et al*, 1999; Xia *et al*, 2002), mitotic exit and cytokinesis (McPherson *et al*, 2004; Yang *et al*, 2004). YAP (a Yorkie homologue) is involved in apoptosis by interacting with p73 (Matallanas *et al*, 2007). Although mutation of WW45 (a Salvador homologue) has been reported in several cancer cell lines (Tapon *et al*, 2002), little is known about the functional significance of WW45 in mammals. So far, only limited biochemical interactions have been reported, including the phosphorylation of LATS1/2 by MST1/2, the

*Corresponding author. National Research Laboratory, Department of Biological Sciences, Korea Advanced Institute of Science and Technology, 373-1 Guseoung-D, Yuseong-G, Daejeon 305-701, Korea. Tel.: +82 42 869 2635; Fax: +82 42 869 2610; E-mail: daesiklim@kaist.ac.kr

Received: 31 October 2007; accepted: 28 February 2008; published online: 27 March 2008

associations of WW45 with MST1/2 and LATS1/2, binding of LATS1 to MOB1 (a MATS homologue) and formation of a complex comprising RASSF1A, MST2, WW45 and LATS1 (Chan *et al*, 2005; Hergovich *et al*, 2006; Guo *et al*, 2007).

The Hippo pathway has also been implicated in mammalian tumorigenesis. Mice lacking LATS1 develop some types of tumour, and hWW45 and Mats are mutated in several cancer cell lines (St John *et al*, 1999; Tapon *et al*, 2002; Lai *et al*, 2005). NF2, the human orthologue of Merlin, is a tumour suppressor gene, mutations of which lead to neurofibromatosis (McClatchey and Giovannini, 2005). YAP is overexpressed in mammalian cancers and transgenic mice overexpressing YAP have an increased liver size and dysplasia with expanded undifferentiated progenitor cells in the intestine (Zender *et al*, 2006; Camargo *et al*, 2007; Dong *et al*, 2007). Of the Hippo pathway proteins, only LATS1-, LATS2-, NF2- and YAP-null mice have been generated; however, these mice are either early embryonic lethal or fail to recapitulate defects seen in the respective *Drosophila* mutants (McClatchey *et al*, 1997; St John *et al*, 1999; McPherson *et al*, 2004, Morin-kensicki *et al*, 2006). Therefore, compared with *Drosophila*, much less is known about the physiological function of the Hippo pathway in mammalian epithelial development. Furthermore, the molecular mechanisms by which this pathway is regulated during development are not fully understood in mammals.

In the present study, we generated mice lacking WW45 to examine the role of the Hippo pathway in mammals. Mutant embryos displayed unchecked proliferation and defects in terminal differentiation of epithelial cells. We also revealed the molecular mechanism by which MST1 signalling is spatiotemporally regulated to allow cell-cycle exit and activation of terminal differentiation in epithelial cells.

Results

Retarded growth and perinatal lethality of the WW45-deficient mice

To identify the role of WW45 *in vivo*, we generated WW45 mutant mice using embryonic stem (ES) cell technology. The targeted mutation replaced a 2.4-kb genomic region containing WW45 exon 2 with a puromycin cassette, leading to premature stop in WW45. After electroporation, the targeted clone was identified and transmitted through the germ line (Figure 1A). The absence of WW45 protein was confirmed by immunoblot assay (Figure 1B). Heterozygous mice were born healthy and fertile, and developed normally. However, only three dwarf homozygotes were found among 954 littermates generated from heterozygous intercrosses, indicating that most of the null mice were embryonic lethal. Viable $WW45^{-/-}$ embryos were found at embryonic days 17.5 (E17.5) and E18.5 (Supplementary Table 1). $WW45^{-/-}$ embryos up to E11.5 were morphologically indistinguishable from their control littermates. However, from about E13.5 onwards, $WW45^{-/-}$ embryos were slightly smaller than the controls, indicating a slower gain in body weight (Figure 1C). Despite growth retardation, we observed no consistent overt defects that would cause the embryonic lethality of mutants. This result prompted us to examine placentas from mutants and their littermates. WW45-null placentas displayed immature development with poor growth and vascularization of the labyrinth layers (Figure 1D). Defective intermingling of fetal and maternal vessels was confirmed by staining with anti-PECAM1 and anti-laminin (Supplementary Figure S1). Thus, the malfunctional labyrinth layer may affect the growth and viability of $WW45^{-/-}$ embryos.

Hyperplasia and immature differentiation of epithelial cells in the WW45-deficient embryos

Previous *Drosophila* studies have proposed important roles for SAV1 in the regulation of proliferation and apoptosis in epithelial tissues. Thus, we performed histological analyses of $WW45^{-/-}$ embryos at various embryonic stages. Interestingly, hyperproliferation of epithelial cells was clearly observed in the skin and intestine (Figures 2 and 3) and other organs (Supplementary Figure S2) of the $WW45^{-/-}$ embryos at E17.5.

We first characterized skin development in these $WW45^{-/-}$ mice. Dividing keratinocytes are normally restricted to the basal layer of wild-type epidermis, and as cells exit from the cell cycle, these keratinocytes move outwards and differentiate to form the spinous layers, the granular layers and the dead enucleated stratum corneum layers at the skin surface (Figure 2Aa). By contrast, the mutant epidermis had a more dense basal layer and the expanded suprabasal layers were less differentiated, with reduced enucleation and compaction of the developing granular cells (Figure 2Aa′). Development of hair follicles was rarely seen, and only small premature hair follicles were seen in null embryos at this stage. Co-staining for E-cadherin and Ki67 revealed that the mutant skin contained increased numbers of proliferative epithelial cells, compared with wild-type skin (Figure 2Ab, b′). Almost all the basal cells and several suprabasal cells expressed Ki67 in the mutant epidermis, whereas proliferation was restricted to the basal layer in the wild-type epidermis. TUNEL (terminal deoxynucleotidyl transferase biotin-dUTP nick-end labelling)-positive cells were also seen in wild-type epidermis but not in mutant epidermis (Figure 2Be, e′). Thus, increased proliferation in the suprabasal layer and repressed apoptosis of terminally differentiated keratinocytes contribute to hyperplasia in the epidermis of mutant embryos.

Epithelia of $WW45^{-/-}$ embryos were hyperproliferative but did not seem to undergo normal differentiation; therefore, we investigated whether epithelial differentiation was delayed and/or defective in mutant epithelia using a panel of antibodies against proteins that are expressed at defined stages of differentiation. Keratin 14 was normally expressed in one or two layers of basal cells in wild-type embryos, whereas it was strongly expressed in the multilayered basal cells in mutant embryos (Figure 2Ba, a′). Moreover, there were increased numbers of keratin-10-expressing cells in the suprabasal layers of the $WW45^{-/-}$ epidermis compared with wild-type embryos (Figure 2Bb′). Expression levels of loricrin and filaggrin, which are markers of late keratinocyte differentiation, were significantly downregulated in mutant epidermis, indicating defects in late differentiation (Figure 2Bc′, d′). Skin-barrier development with X-gal staining further confirmed the absence of terminally differentiated layers (Supplementary Figure S3). Electron microscopy analysis clearly showed that the epidermis of WW45-null embryos was thicker than the wild-type epidermis. Moreover, the granular and cornified layers present dysmaturation in the mutant epidermis, with nucleated cells reaching the epidermal surface (Figure 2C). These data indicate that the

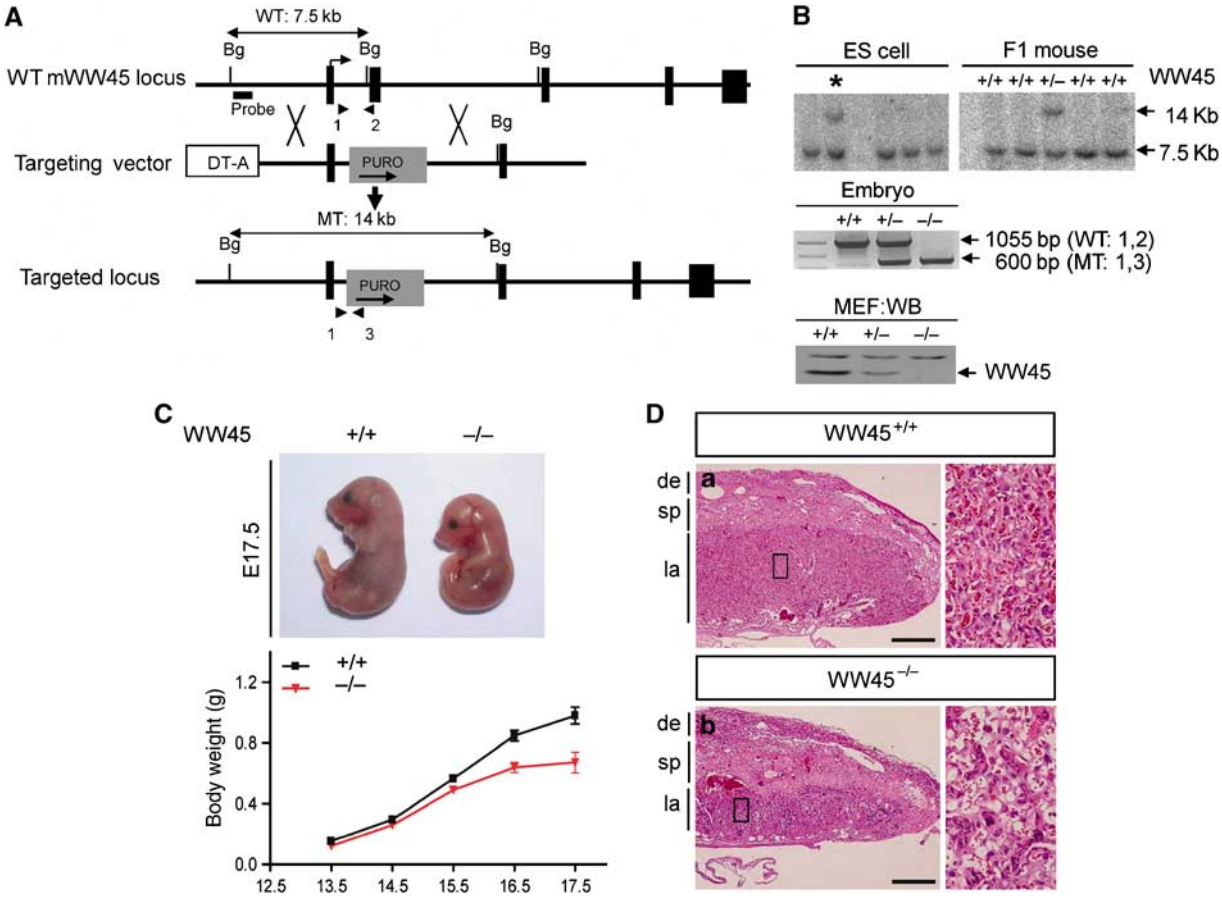

Figure 1 Targeted disruption of the WW45 gene by homologous recombination. (**A**) Schematic representation of the WW45 targeting strategy, showing the mouse WW45 genomic locus, targeting vectors and targeted locus. Exon 2 was replaced with a puro cassette, and diphtheria toxin A was used for negative selection. Five exons are indicated by black boxes. Also indicated are the 5′-external probe for Southern hybridization of genomic DNA, predicted sizes of fragments with restriction sites and primer pairs for PCR. Arrowheads represent primers used for genotyping of the WT (1 and 2) or MT (1 and 3) alleles. Bg, *Bgl*II restriction site. (**B**) Southern blot analysis of genomic DNA digested with the restriction enzyme *Bgl*II using the 5′ probe, and PCR genotype analysis of embryos. Western blot analysis (WB) shows the presence of WW45 in cultured primary fibroblasts. The arrow indicates bands of WW45. (**C**) Growth retardation of mutant (−/−) WW45 embryos. Appearance of wild-type and mutant embryos at E17.5 (top). Growth curves of wild-type (+/+) and mutant (−/−) WW45 embryos (bottom). (**D**) Haematoxylin and eosin (H&E)-stained sections of placentas from E17.5 embryos. Note that the major layers had defective maturations with reduced and disordered vasculature in mutant placentas. de, decidua; sp, spongiotrophoblast layer; la, labyrinth layer. Scale bar: 500 μm. Boxed regions are shown at high magnification.

suprabasal mutant keratinocytes fail to stop proliferating and terminally differentiate.

We also examined intestinal development in mutant embryos. Wild-type intestinal epithelium consists of a monolayer of polarized epithelial cells organized into crypts. By contrast, the mutant epithelium was multilayered and displayed hypercellularity with pseudostratified and enlarged nuclei, perturbed differentiation with loss of goblet cells and increased numbers of mitotic cells (Figure 3Aa′ and Supplementary Figure S2a, a′). Furthermore, Ki67 staining revealed extensive proliferation throughout the villus epithelium in the small intestine, whereas proliferative cells were restricted to the crypt bases in the control epithelium (Figure 2Ab, b′). Indeed, all epithelial cells in the mutant colons were Ki67-positive, indicating dysplasia (Supplementary Figure S4A). In agreement with these results, bromodeoxyuridine (BrdU) pulse experiments further confirmed significantly increased numbers of dividing cells in mutant epithelia of many organs (Supplementary Figure S4B).

We then examined differentiation of the various intestinal epithelial cell lineages. During differentiation of enterocytes, the FABP protein was detected at normal levels in the villi of wild-type embryos but at markedly reduced levels in the mutant embryos (Figure 3Ba, a′). Similarly, chromogranin labelling, which detects differentiation along the entero-endocrine lineage, was rarely detected in mutant embryos (Figure 3Bb, b′). Staining with Alcian blue, a marker for goblet cells, revealed a complete absence of muco-secreting goblet cells in all mutant intestinal tracts (Figure 3Bc, c′). Ultrastructural analysis also revealed poorly developed microvillus brush borders on the apical surfaces of the villous enterocytes, indicating defective enterocyte differentiation in the mutant epithelium of the small intestine (Figure 3C). Interestingly, these mutant cells had enlarged nuclei located close to the apical region, indicating a loss of apical–basal polarity.

In addition to immature differentiation of the mutant skin and intestine, immature differentiation was also detected in the lungs of mutant embryos (Lee and Lim, personal observation). Taken together, these results indicate that WW45 deficiency induces hyperplasia and immature differentiation in epithelial tissues.

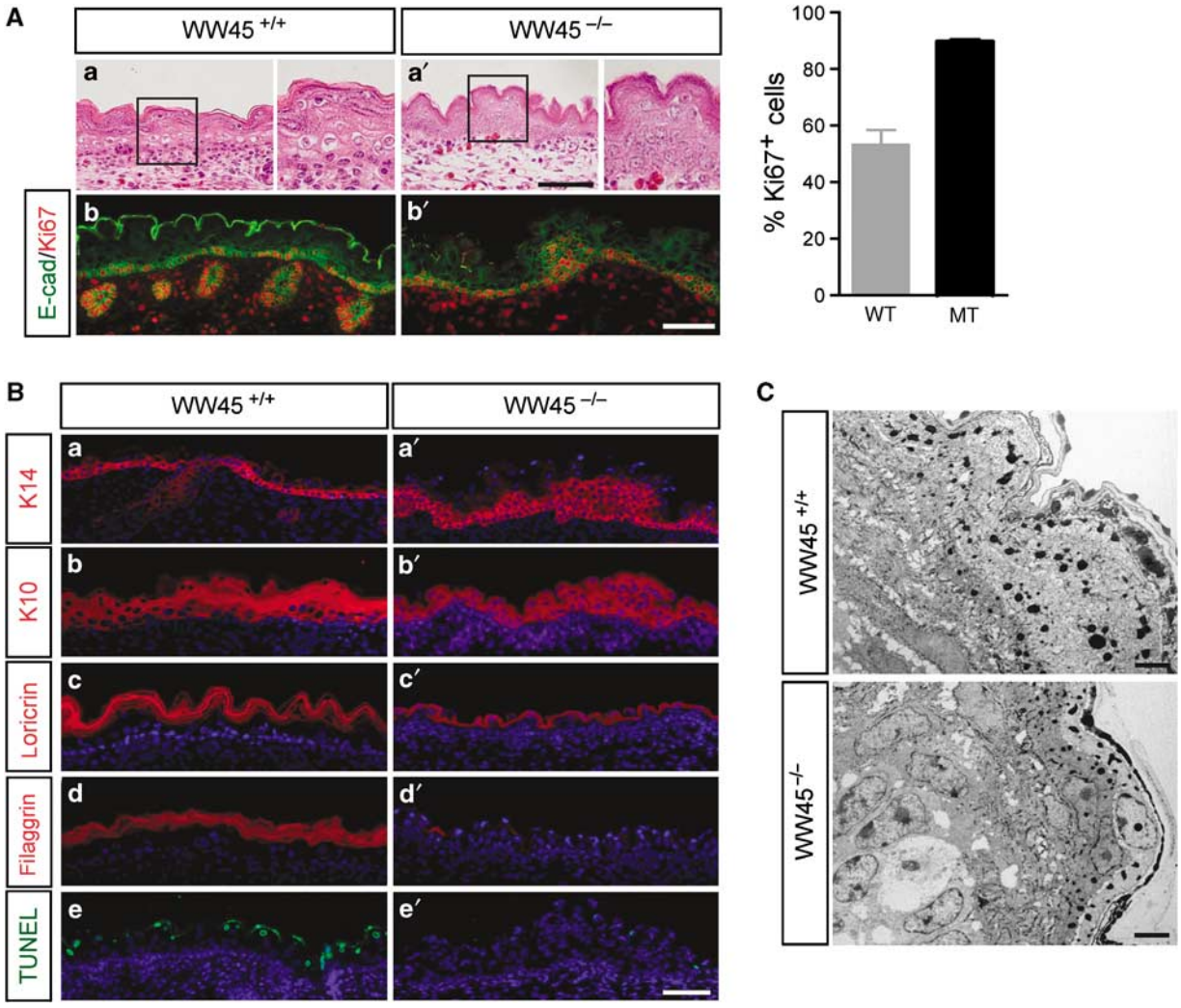

Figure 2 Hyperproliferation and immature differentiation in WW45$^{-/-}$ epidermis at E17.5. (**A**) H&E-stained sections of wild-type (a) and mutant (a′) epidermis. Evaluation of cellular proliferation was conducted by co-immunohistochemistry analysis with anti-Ki67 and anti-E-cadherin (b, b′). Note the increased numbers of Ki67-positive cells, including in multiple cell layers, in the mutant epidermis. Quantitation of the percentage of proliferating cells per 1 mm^2 area in mutant versus control epithelium from three independent experiments (±s.d.). Boxed regions are shown at high magnification in the right panel of each genotype. WT, wild type; MT, mutant. (**B**) Differentiation marker expression in the skin of wild-type or mutant embryos. Immunohistochemistry analysis was performed with antibodies against K14, K10, loricrin and filaggrin, in addition to TUNEL staining for analysis of apoptosis. 4′,6-diamidino-2-phenylindole (DAPI)-stained nuclei are shown in blue. Note the lack of stratification and differentiation and the increased numbers of progenitor cells in the mutant epidermis. (**C**) Electron microscopy analysis of the wild-type (upper panel) and mutant (lower panel) epidermis. Note the loss of columnar morphology in basal cells and the disorganized suprabasal cells, as well as the loss of flattened granular and cornified layers in the mutant skin. Scale bar: 100 μm (A, B), 2 μm (C).

WW45 regulates cell-cycle exit in epithelial progenitor cells during differentiation

We tested whether excessive proliferation of mutant cells was due to increased proliferation rates or failure of cell-cycle exit for terminal differentiation. First, we examined the cell-cycle duration in epithelial progenitor cells by analysing the proportion of cycling cells (Ki67$^+$) in S-phase 1 h after injection of BrdU (Schmahl, 1983). Although the percentage of BrdU-labelled cells was increased in mutant embryos, the BrdU$^+$Ki67$^+$/Ki67$^+$ labelling index was approximately the same in wild-type and mutant embryos, indicating similar proliferation rates in wild-type and mutant embryos (Figure 4A). Second, we determined the frequency of cell-cycle re-entry by assessing the proportion of dividing cells (BrdU$^+$) 24 h after BrdU injection (Chenn and Walsh, 2002). During the time interval between BrdU application and analysis, cells can leave (Ki67$^-$) or re-enter the cell cycle (Ki67$^+$). The mean ratio of BrdU$^+$Ki67$^+$/BrdU$^+$ cells was significantly increased by 49% in the mutant small intestine and by 58% in the mutant colon compared with wild-type controls (Figure 4B), indicating that WW45 promotes exit from the cell cycle in epithelial progenitors during embryonic development.

Failure of cell-cycle exit of WW45$^{-/-}$ keratinocytes during in vitro differentiation

To further analyse the rates of proliferation and differentiation of epithelial cells, we isolated primary keratinocytes from the skin of embryos. Consistent with *in vivo* data (Figure 4A), WW45$^{-/-}$ keratinocytes had normal cell-cycle distribution and the rate of proliferation was not significantly increased compared with control cells (Figure 4C and data not shown).

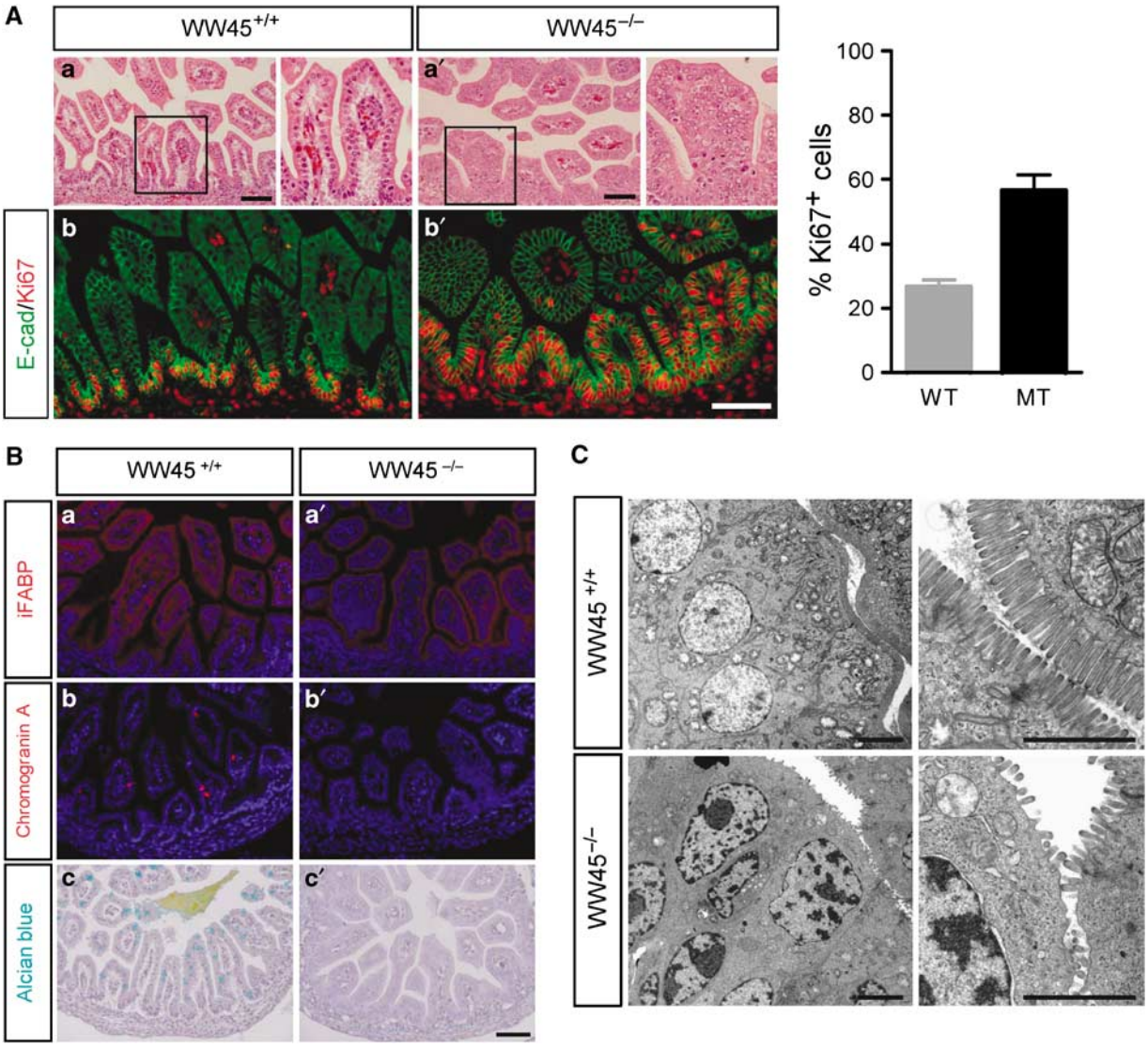

Figure 3 Hyperplasia and immature differentiation of WW45$^{-/-}$ intestinal epithelium at E17.5. (**A**) H&E-stained sections of wild-type (a) and mutant (a′) intestine. Immunostaining analysis with anti-Ki67 and anti-E-cadherin (b, b′). Note the increased numbers of Ki67-positive cells, including in multiple cell layers, in the mutant epithelium. Quantitation of the percentage of proliferating cells per 1 mm^2 area in epithelium from three independent experiments (±s.d.). Boxed regions are shown at high magnification in the right panel of each genotype. WT, wild type; MT, mutant. (**B**) Differentiation marker expression in the intestine of wild-type or mutant embryos. Immunohistochemistry analysis was performed with indicated antibodies, in addition to Alcian blue staining. Note the significant reductions in the levels of terminal differentiating cells, goblet cells and entero-endocrine cells in mutants compared with wild-type littermates. (**C**) Electron microscopy analysis of the wild-type (upper panel) and mutant (lower panel) intestines. Note the reduced density of brush-border microvilli of mutant enterocytes compared with the densely compacted, uniformly distributed microvilli of wild-type enterocytes. Scale bar: 100 μm (A, B), 2 μm (C).

Again, this suggests that WW45 is unlikely to regulate the rate of proliferation. We then examined the ability of WW45 to regulate proliferation arrest and differentiation of developing epidermal cells by adding calcium, transforming growth factor (TGF)-β or LiCl, which have been shown to induce proliferation exit, and possibly terminal differentiation, of keratinocytes (Hennings *et al*, 1980; Shipley *et al*, 1986; Olmeda *et al*, 2003). With Ca^{2+}, TGF-β or LiCl treatment, the wild-type cells showed efficient growth arrest and the numbers of BrdU-labelled cells were reduced. By contrast, mutant cells continued to proliferate and were BrdU-positive 24 h after Ca^{2+}, TGF-β or LiCl treatment (Figure 4D and Supplementary Figure S5). Consistently, the expression of filaggrin was evident in wild-type but not in mutant keratinocytes after induction of differentiation (Figure 5A). These data indicate that increased proliferation in WW45$^{-/-}$ epithelial tissues results from impaired growth arrest of progenitor cells during differentiation rather than from an increased rate of proliferation.

Activation of the MST signalling pathway during keratinocyte differentiation in vitro

To further characterize the molecular mechanisms by which WW45 regulates cell-cycle exit during differentiation, we investigated the phosphorylation and localization of MST, LATS and YAP in keratinocytes during differentiation. Interestingly, autophosphorylation of MST1 was induced upon differentiation, as shown by phospho-MST1 immunoblotting, indicating MST1 activation (Figure 5A). By contrast, this autophosphorylation of MST1 was not detected in

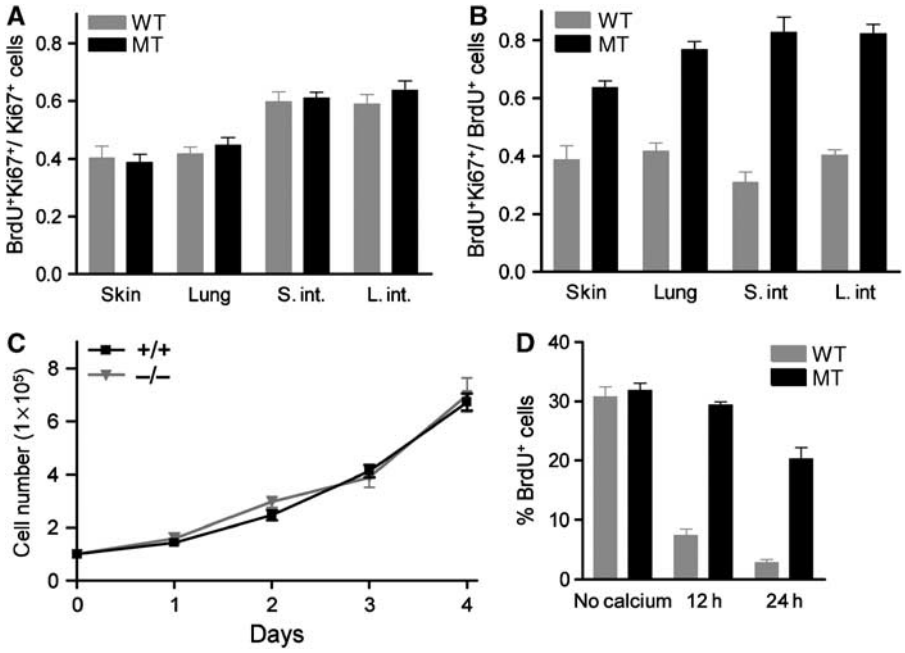

Figure 4 Increased numbers of cycling cells in the developing $WW45^{-/-}$ epithelium resulted from inefficient growth arrest. (**A**) The proportion of progenitor cells ($Ki67^{+}$) labelled with BrdU after a 1 h pulse. There is no difference in cell-cycle length between wild-type and mutant embryos. (**B**) Analysis of immunoreactivity for Ki67 in BrdU-positive cells 24 h after BrdU injection. The fraction of cells re-entering the cell cycle ($BrdU^{+}Ki67^{+}$) is significantly increased in mutant embryos. (**C**) Growth curves of primary keratinocytes isolated from wild-type and mutant epidermis show similar proliferation rates. (**D**) Induction of calcium-stimulated differentiation in primary keratinocytes. The level of BrdU incorporation in keratinocytes cultured in the absence or presence of Ca^{2+} for the times indicated is shown. The mutant keratinocytes show inefficient growth arrest under differentiation conditions. (A–D) Data represent triplicate independent experiments ($\pm$s.d.).

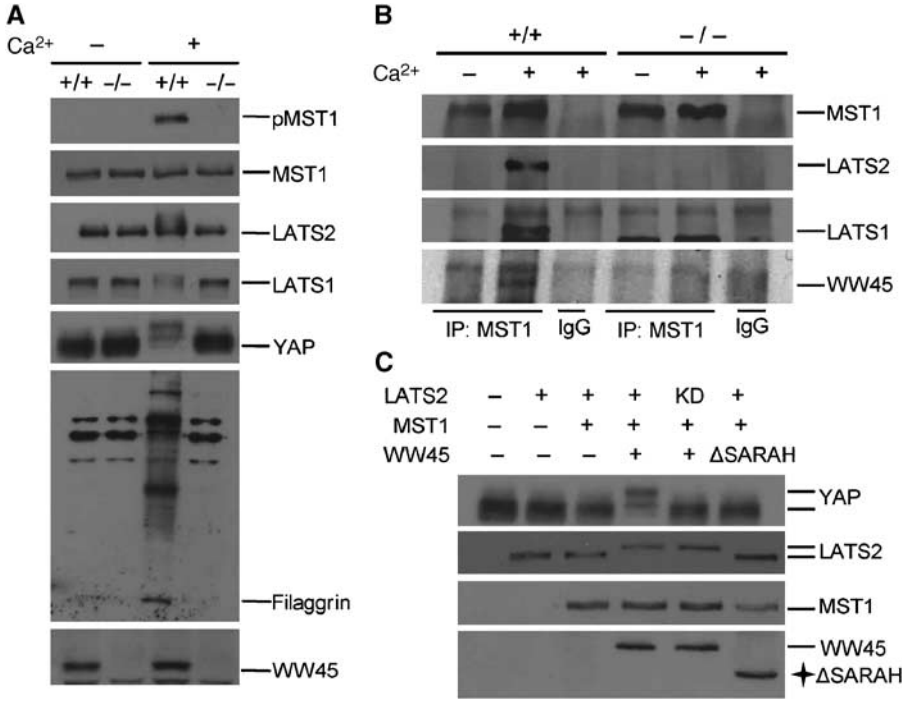

Figure 5 Activation of MST1 signalling pathway during differentiation. (**A**) Protein status of components of the MST1 pathway under differentiation conditions. Primary keratinocytes were incubated with or without Ca^{2+} for 24 h and analysed by western blot analysis with the indicated antibodies. Note the activation of MST1, as shown by pMST1 blotting, and the mobility shift of YAP and LATS1/2 in the control keratinocytes, but not in mutant keratinocytes, under differentiation conditions. Keratinocyte differentiation was confirmed by western blot analysis of filaggrin expression. (**B**) Wild-type and mutant primary keratinocytes cultured with or without Ca^{2+} for 24 h were analysed by immunoprecipitation with anti-MST1 and by western blot assays. Note that complex formation is only detected with Ca^{2+} treatment in the control samples. (**C**) Phosphorylation of YAP by activated LATS2 through MST1/WW45. $WW45^{-/-}$ primary keratinocytes were co-transfected with the indicated plasmids and probed with the indicated antibodies. Note the mobility shift of YAP and LATS2 in the presence of MST1 and intact WW45.

mutant cells. Therefore, WW45 is required for MST1 activation after induction of differentiation with calcium treatment. In addition, the mobility patterns of LATS1/2 and YAP differ after induction of differentiation with calcium treatment (Figure 5A). Phosphorylation of LATS1/2 and YAP was detected in differentiated wild-type keratinocytes, but not in differentiated mutant keratinocytes. Thus, phosphorylation of YAP seems to be dependent on the MST1 signalling pathway, in particular on LATS1/2, during epithelial differentiation in mammals.

We then investigated whether the formation of components of the MST1 signalling pathway might be associated with and affect differentiation of keratinocytes. We first transfected WW45$^{-/-}$ keratinocytes with LATS1/2, MST1 and YAP with or without WW45, and then induced differentiation before immunoprecipitation. In mutant keratinocytes, LATS1and LATS2 co-precipitated with YAP but not with MST1. By contrast, these proteins form a stable complex in the presence of WW45 (Supplementary Figure S6). Moreover, endogenous MST1 and LATS1/2 formed a complex in keratinocytes under differentiated conditions and in the presence of WW45 (Figure 5B). In addition, YAP was fully phosphorylated in keratinocytes complemented with wild-type WW45 and expressing LATS2 wild type, but not in cells with wild-type WW45 and expressing LATS2 kinase dead (KD) and MST1 or in cells complemented with WW45 lacking the SARAH domain, which is responsible for interaction with MST1 (Figure 5C). These results indicate that, in mammals, WW45 is required for MST1 activation and promotes LATS1/2 phosphorylation by recruiting MST1 into the complex, and that activated LATS1/2 then phosphorylates YAP. Surprisingly, activation of the MST1 signalling pathway in mammals seems to be specific for differentiation signals, at least for keratinocyte differentiation.

We next found that the serine 127 of YAP was phosphorylated by LATS1/2 *in vitro* and *in vivo* (Supplementary Figure S7). This result is consistent with the recent finding that serine 127 of YAP is the primary Hippo-responsive phosphorylation site (Dong *et al*, 2007). We further confirmed that this is a phosphorylation site of endogenous YAP with a phosphoserine 127 antibody during keratinocyte differentiation (Supplementary Figure S7).

Dynamic cellular localizations of MST1 and YAP during epithelial differentiation

YAP associates with the Src family kinase at the plasma membrane, with 14-3-3 family proteins in the cytoplasm and with transcription factors in the nucleus, suggesting a dynamic localization of YAP in cells (Sudol, 1994; Yagi *et al*, 1999; Vassilev *et al*, 2001; Matallanas *et al*, 2007). However, the localization of other components of MST1 pathway has not been determined. Thus, we examined the subcellular localization of MST1 pathway components during epithelial cell differentiation by nuclear-cytoplasmic fractionation experiments. MST1 was mainly detected in the cytoplasmic fraction under undifferentiated conditions, but a significant amount was detected in the nuclear fraction after differentiation induction in wild-type cells, suggesting that differentiation triggered MST1 translocation to the nucleus. However, this nuclear localization of MST1 was severely compromised in mutant cells (Figure 6A). We also found that YAP was found mainly in the nucleus under undifferentiated conditions, but it was phosphorylated and mainly detected in the cytoplasm of differentiated wild-type cells. However, cytoplasmic localization and phosphorylation of YAP were compromised in mutant cells under differentiated conditions (Figure 6A). These results indicate that induction of keratinocyte differentiation triggers translocation of MST1 into the nucleus and then activates LATS1/2, which in turn phosphorylates YAP, and that WW45 is necessary for this. We further examined the ability of MST1/WW45/LATS2 to modulate the localization of YAP by ectopically overexpressing these proteins in mutant keratinocytes. Consistent with previous results, YAP was phosphorylated by LATS2 and this phosphorylated form was found in the cytoplasm, probably owing to nuclear translocation of MST1 by WW45 (Figure 6B). By contrast, these dynamic localizations of MST1 and YAP were not seen in cells expressing WW45 lacking the SARAH domain, which indicates that the WW45 SARAH domain is required for this process. Moreover, the YAP S127A mutant was mainly localized to the nucleus regardless of MST1 signalling activation, indicating that phosphorylation of serine 127 of YAP by LATS2 in the nucleus promotes translocation of YAP into the cytoplasm.

We also examined the distinct localization of MST1 and YAP by performing an immunostaining assay in differentiated keratinocytes as well as embryo tissue sections (Figure 6C and D). The specificity of MST1 antibody was assessed by immunoblot and immunostaining analyses with MST1-depleted cells (Supplementary Figure S8). Consistent with the fractionation results, we also observed dynamic translocation of endogenous YAP and MST1 during differentiation in the wild-type cells but such translocation was not apparent in the mutant cells during differentiation (Figure 6C). Moreover, although phosphorylated YAP was evidently found in the cytoplasm in differentiated wild-type cells, it was barely detectable in mutant cells. In wild-type tissue sections, we detected nuclear-localized YAP in proliferative basal cells, which were Ki67-positive, and cytoplasm-localized YAP in differentiated cells (Figure 6D and Supplementary Figure S9). This result is consistent with the recent finding that YAP is expressed and localized in the nuclei of the crypt compartment of the small intestine (Camargo *et al*, 2007). However, MST1 was detected in the cytoplasm of proliferating cells, but in the nucleus of differentiated cells in the wild-type skin and intestine. By contrast, many proliferating cells of mutant embryos showed cytoplasm-localized MST1 and nuclear-localized YAP (Figure 6D). In addition to changes in MST1 and YAP localizations, the cytoplasm of the differentiated regions in control embryos stained positive for phosphor-YAP, but staining levels were significantly reduced in mutant embryos (Figure 6D). Therefore, consistent with *in vitro* epithelial differentiation results, the changes in the dynamic localization of MST1 and YAP are also likely to occur as epithelial cells undergo differentiation *in vivo*, and WW45 is likely to be a key protein in this process.

The failure of proliferation arrest and differentiation of normal keratinocytes expressing YAP S127A

We next assessed whether the phosphorylation of serine 127 of YAP is required for inducing keratinocyte growth arrest and differentiation. Thus, keratinocytes were infected with a retrovirus expressing YAP wild type, YAP S127A, which is a non-phospho form, or YAP S127D, which is a phospho-mimic

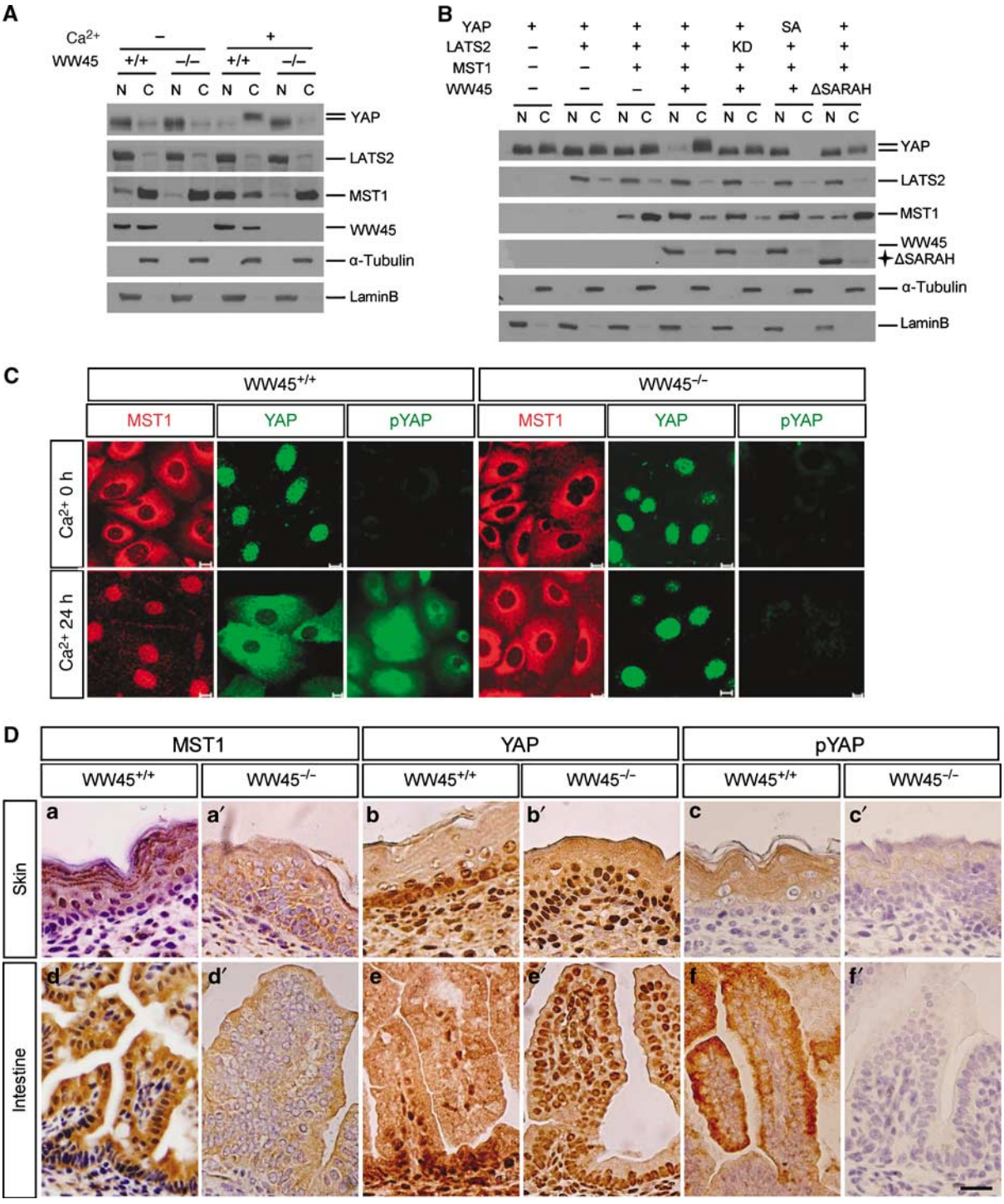

Figure 6 Dynamic localization of MST1/YAP during differentiation. (A–C) Subcellular localization of MST1 and YAP in response to differentiation stimuli. (**A**) Fractionation experiments were conducted with primary keratinocytes from wild-type or mutant embryos with or without Ca^{2+} for 24 h. Fractionated lysates were subjected to western blot analysis with the indicated antibodies. N, nuclear; C, cytoplasmic. (**B**) WW45-deficient keratinocytes were co-transfected with the indicated plasmids. After 24 h of transfection, cells were maintained in Ca^{2+} medium for a further 24 h before harvesting for fractionation experiments. Western blot analysis was performed with the indicated antibodies. Note that the major cytoplasm translocation of YAP and nuclear translocation of MST1 were detected only in the presence of intact WW45. (**C**) Primary keratinocytes were cultured with or without Ca^{2+} for 24 h and then subjected to immunostaining with anti-MST1, anti-YAP and anti-p-YAP. Note the phospho-dependent translocation of YAP and MST1 in Ca^{2+}-induced differentiated control cells but not in mutant cells. (**D**) Immunoperoxidase staining for MST1, YAP and p-YAP in wild-type (a–f) and mutant (a′–f′) epithelium at E17.5. Note the intense nuclear detection of YAP and cytoplasmic detection of MST1 in most mutant epithelial cells, which is in contrast to the dynamic distributions according to differentiation stage in control epithelial cells. Serine 127 phospho-specific immunoreactivity was cytoplasm-specific in the differentiating zones in the control, whereas the signal was absent from the mutant cells. Counterstaining was performed with haematoxylin. (a–c, a′–c′) Skin; (d–f, d′–f′) small intestine. Scale bar: 10 μm (C) and 100 μm (D).

form. Calcium-induced differentiation signals suppressed proliferation of growing keratinocytes expressing YAP wild type or YAP S127D. By contrast, YAP S127A was mainly localized to the nucleus and its overexpression in wild-type cells failed to cause proliferation arrest and differentiation (Figure 7A–C). These results indicate that YAP S127A is localized to and acts in the nucleus to allow cells to proliferate even in the presence of differentiation signals. We also tested whether inactivation of YAP suppresses the differentiation defect in WW45-deficient keratinocytes. To do this, we generated the dominant-negative form of YAP (DN), which dominantly inhibits the function of endogenous YAP protein (Zhao *et al*, 2007). Importantly, YAP DN was sufficient to rescue the differentiation of mutant cells (Figure 7D and E). Taken together, these results show that inactivation and subcellular targeting to the cytoplasm of phosphorylated YAP is required for cell-cycle exit and differentiation initiation.

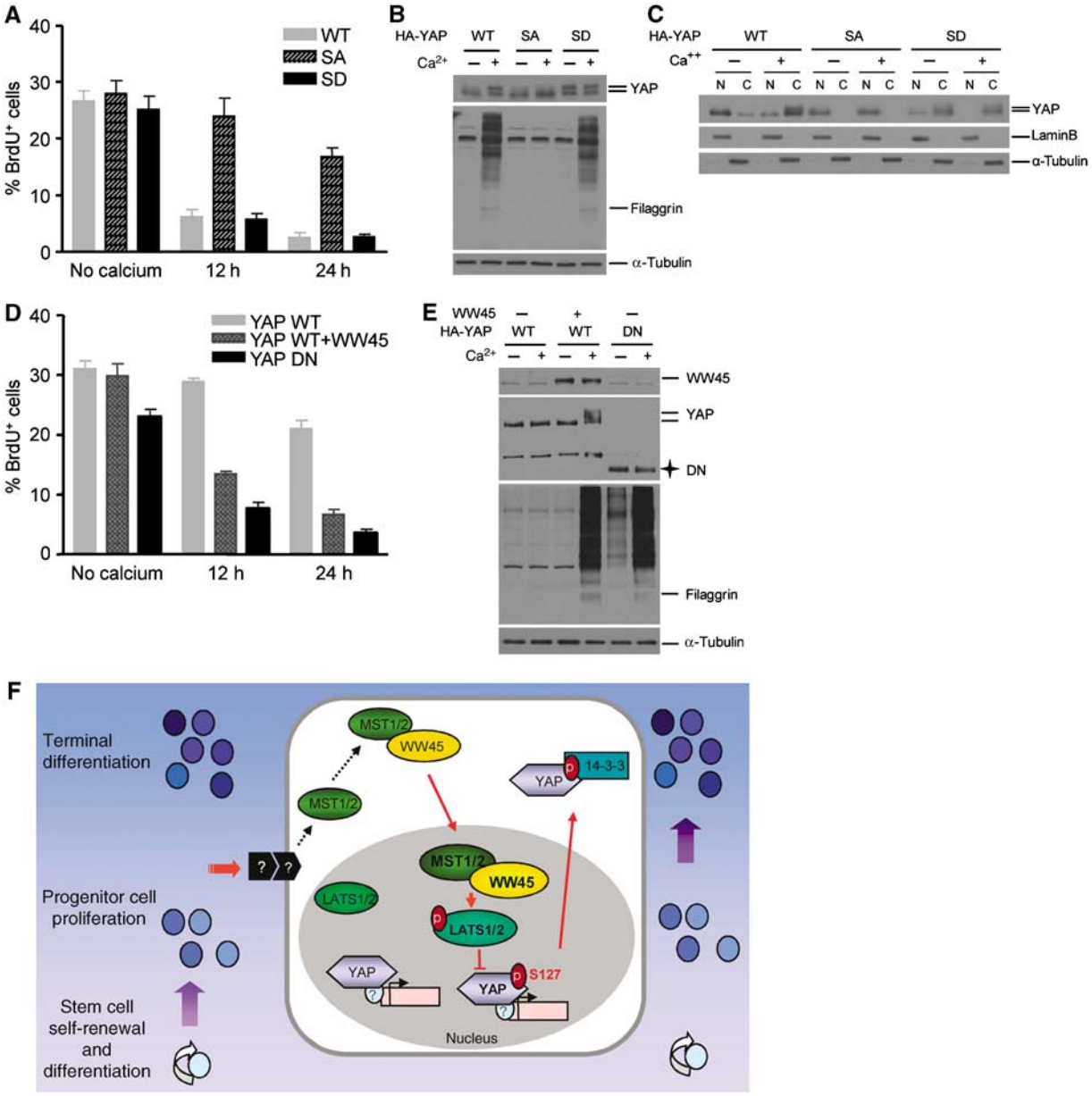

Figure 7 Effects of phosphorylation of YAP serine 127 on epithelial differentiation. (**A**) The percentage of proliferative cells labelled with BrdU under differentiation conditions. Levels of BrdU incorporation in primary keratinocytes were determined at the indicated times after retroviral infection with the indicated genes and incubation with or without Ca^{2+}. WT, wild type; SA, S127A mutant; SD, S127D mutant. Note the failure of cell-cycle exit in response to Ca^{2+}-induced differentiation in YAP-SA-infected cells. (**B**) Failure of YAP-SA-infected cells to differentiate in response to differentiation stimuli. Lysates from (A) were subjected to western blot analysis with the indicated antibodies. Note the suppression of YAP mobility shift in the absence of processed forms of filaggrin in YAP-SA-infected cells. (**C**) Subcellular localization of YAP, YAP SA and YAP SD in response to differentiation stimuli. Fractionations from (A) were subjected to immunoblot analysis. Note the lack of cytoplasmic translocation of YAP SA under Ca^{2+}-induced differentiation conditions. (**D**) The percentage of BrdU-positive cells in mutant keratinocytes infected with the indicated genes under differentiation conditions. WT, wild type; DN, dominant-negative form. Note the suppression of cell-cycle re-entry in response to Ca^{2+} treatment in mutant keratinocytes infected with YAP-DN. (**E**) Lysates from (D) were subjected to western blot analysis with the indicated antibodies. Note the rescue of differentiation in response to Ca^{2+} treatment in mutant keratinocytes infected with YAP-DN. (**F**) Proposed model for the role of WW45 in developing epithelial tissues.

Discussion

This study provides novel insights into the role of WW45 in mammalian epithelial tissue development. WW45 is a key regulator of the MST1 signalling pathway, which promotes cell-cycle exit and terminal differentiation in developing epithelial tissues. Ablation of WW45 leads to hyperproliferation accompanied by immature differentiation in epithelial cells of the skin and intestine (Figures 2 and 3), and this phenotype results from re-entry of differentiating cells into the cell cycle rather than intrinsic acceleration of proliferation (Figure 4). This conclusion is strongly supported by our observations that WW45-null primary keratinocytes cannot be efficiently induced to exit the cell cycle in response to differentiation signals such as Ca^{2+}, TGF-β or LiCl, and that increased proliferation rates were detected from E15.5 onwards, which is the onset of terminal differentiation events in the epithelium (Figure 4 and Supplementary Figures S10 and S11). The Hippo pathway has been implicated in the restriction of proliferation and promotion of apoptosis in epithelial cells, but there is little evidence that this pathway is involved in terminal differentiation in *Drosophila*. Interestingly, the mouse MST1 signalling pathway seems to have a role in terminal differentiation in the developing epithelial tissues.

Previous studies with *Drosophila* have identified several genes and their interactions in the Hippo pathway (Edgar, 2006; Harvey and Tapon, 2007; Pan, 2007); however, the intracellular signalling of spatiotemporal regulation during epithelial differentiation remains unclear. This study determines the underlying mechanism by which components of the MST1 signalling pathway spatiotemporally regulate cell-cycle exit for epithelial differentiation in mammals. We show that as yet unknown differentiation signals specifically activate the MST1 kinase, which then dynamically localizes to the nucleus and activates LATS1/2, and that WW45 is required for this process. Activated LATS1/2 then phosphorylates serine 127 of YAP, and this phosphorylated YAP localizes to the cytoplasm where it is inactivated (Figure 7F). Recently, the serine 127 of YAP has been shown to be the main phosphorylation site in the Hippo pathway and its phosphorylation results in its cytoplasmic translocation (Dong *et al*, 2007); overexpression of YAP in mice induces a severe dysplasia accompanied by expansion of multipotent undifferentiated progenitor cells in the skin and intestine (Camargo *et al*, 2007). These phenotypes are quite similar to those seen in WW45-null embryos. Here, we have shown that phosphorylation of serine 127 of YAP by LATS1/2 in MST signalling occurs during epithelial differentiation. Based on our observations, we propose a hypothesis that, during formation of mature epithelial tissues in mammals, the MST1 pathway is activated by differentiation signals and determines when precursor cells stop dividing and terminally differentiate, and that WW45 may be central to this process (Figure 7F). Interestingly, transgenic mice overexpressing YAP S127A in the liver displayed enlarged livers (Camargo *et al*, 2007; Dong *et al*, 2007), supporting the hypothesis that Hippo signalling regulates mammalian organ size. However, no organs of increased size were seen in $WW45^{-/-}$ embryos, which could be due to placental defects or another genetic compensation. Thus, tissue-specific or conditional knockout experiments in mice are required for further clarification of the role of the MST1 pathway in regulation of organ size in mammals.

Recent studies in *Drosophila* have indicated that, together with cyclin E, Diap1 and bantam may be additional targets of Yorkie (Nolo *et al*, 2006; Thompson and Cohen, 2006). However, unlike in *Drosophila*, no direct target genes were identified in the MST1 pathway. Of interest, quantitative RT–PCR revealed that, although slightly increased, expression levels of cyclin E, cIAP, XIAP and survivin were not significantly upregulated in $WW45^{-/-}$ cells, indicating that other targets of YAP control developmental homeostasis in mammalian epithelial tissues (Supplementary Figure S12). Based on our observation that YAP DN is sufficient to rescue the cell-cycle exit and differentiation of $WW45^{-/-}$ cells, identification of the downstream targets or mediators of YAP will provide important insights into how YAP could control both cell-cycle exit and terminal differentiation.

We also found that WW45 deficiency led to disruption of contact inhibition of proliferation (data not shown), as is also seen with loss of LATS2 and NF2 (Lallemand *et al*, 2003; McPherson *et al*, 2004; Okada *et al*, 2005). WW45 is also likely to participate in the contact inhibition signalling pathway. Loss of contact inhibition might be associated with the hyperplasia observed in epithelial tissues of $WW45^{-/-}$ embryos. Recently, inactivation of YAP in the Hippo pathway has been shown to contribute to cell contact inhibition and tissue growth (Zhao *et al*, 2007). Thus, further studies should investigate whether defects in contact inhibition in $WW45^{-/-}$ cells are due to a failure of YAP inactivation.

Perturbations in MST1 signalling lead to inappropriate proliferation and expansion of cell compartments, which in turn lead to increased risks of cancer-associated mutations. Several results support the importance of the Hippo pathway in mammalian tumorigenesis. Loss of expression of LATS1/2, hWW45 and Mats has been reported in cancer cell lines (Tapon *et al*, 2002; Lai *et al*, 2005; Takahashi *et al*, 2005; Jiang *et al*, 2006). Mice with mutations in LATS1or NF2 develop tumours, and *YAP* transcription is increased in the mouse tumour model (St John *et al*, 1999; McClatchey and Giovannini, 2005; Zender *et al*, 2006). Moreover, YAP can transform immortalized mammary epithelial cells *in vitro* and transgenic mice overexpressing YAP develop liver cancers or intestinal dysplasia with loss of differentiated cell types (Overholtzer *et al*, 2006; Camargo *et al*, 2007; Dong *et al*, 2007). In addition to these reports, this study revealed that dysfunction of a single gene, WW45, affects most developing epithelial tissues and induces characteristics of a precancerous state: uncontrolled proliferation, partial loss of epithelial polarity and block of terminal differentiation. However, no such phenotypes have been reported in mice lacking LATS1, LATS2 and NF2. Multiple homologues of the fly Hippo pathway exist in mammals; hence, there may be functional redundancy of these proteins. However, WW45 is the only mammalian homologue of the Sav in the Hippo pathway, and its loss led to marked phenotypic changes in many epithelial tissues. Importantly, we found that, during a 14-month observation period, 22% of WW45 heterozygous mice developed some type of tumour including osteosarcoma and hepatoma (Lee and Lim, personal observation). Therefore, future studies should investigate how the heterozygous status of WW45 initiates tumorigenesis and the molecular characteristics of developed tumours in these mice. Finally, WW45-knockout embryo or WW45 heterozygous mice could be a suitable model for tumorigenesis studies of the MST1 pathway.

Materials and methods

Generation of WW45-null mice

$WW45^{-/-}$ mice were generated using standard ES cell (R1) homologous recombination and blastocyst injection techniques. A targeted ES cell clone was injected into C57BL/6 blastocysts to generate germline-transmitting chimaeric mice. Mice and ES cells were genotyped by PCR assays with primers WW45-L (TGACC ATGTGTCCAGCCTTA), WW45-R (CGAATGGATGCTGCATATTG) and pGK-3 (GCACGAGACTAGTGAGACGTGCTAC).

Histological analysis

Embryos were fixed in 4% paraformaldehyde and embedded in paraffin. Sections (4 μm) were stained with H&E or subjected to immunohistochemical analysis. Immunohistochemical analysis was performed using standard protocols with antibodies against PECAM-1, laminin (Abcam), BrdU, E-cadherin, β-catenin (BD), Ki67 (Novocastra), anti-filaggrin, loricrin, K10, K14, K1 (Covance), iFABP (gift from Dr JI Gordon), chromogranin A (Immunostar), YAP (Cell Signaling, Santa Cruz), and p-YAP (Cell Signaling). Peroxidase levels were assessed using the EnVision® + Dual Link System-HRP(DAB +) (DakoCytomation). Intestinal goblet cells were stained with Alcian blue to detect mucin. The TUNEL assay was performed using a commercial staining kit (Roche). BrdU incorporation experiments were performed by injecting pregnant females intraperitoneally with BrdU (Sigma) at a concentration of 100 μg per g body weight. At 1, 2 or 24 h after injection, embryos were dissected and fixed for immunohistochemical analysis.

Electron microscopy

Electron microscopy analysis of tissue samples was performed according to standard protocols. Briefly, samples were fixed with 3% glutaraldehyde for 2 h and then washed with 0.1 M cacodylate buffer containing 0.1% $CaCl_2$. Samples were then post-fixed with 1% OsO_4 in 0.1 M cacodylate buffer (pH 7.2) containing 0.1% $CaCl_2$ for 2 h at 4°C. After dehydration in graded alcohol concentrations, the cells were embedded in Spurr's epoxy resin. After polymerization of the resin at 70°C for 36 h, serial sections were cut and mounted on formvar-coated slot grids. Sections were stained with 4% uranyl acetate for 10 min and with lead citrate for 7 min. A Tecnai G2 Spirit Twin transmission electron microscope (FEI Company, USA) and a JEM ARM 1300S high-voltage electron microscope (JEOL, Japan) were used.

Plasmid construction

Human cDNAs for WW45, MST1, LATS1/2 and YAP were cloned into pDK-Flag2 or pCMV-HA (HA: haemagglutinin), which had been modified from pcDNA3.1 or pcDNA3 (Invitrogen). Site-directed PCR mutagenesis was used to introduce the missense changes S127A and S127D into the YAP sequence. The S127A nuclear-localizing form with a deletion of the C-terminal TA domain of YAP was generated and used for YAP-DN mutant form.

Generation of antibodies

Rabbit polyclonal antibodies to MST1 were prepared with purified recombinant hexahistidine (His_6)-tagged MST1(K59R) as the antigen and then affinity purified and used for immunostaining. Rabbit polyclonal antibodies to WW45 (Rb Ctr#1) were generated by injecting rabbits with a keyhole-limpet-haemocyanin-conjugated peptide corresponding to the 14 C-terminal amino acids of mouse WW45 (RKQRQQWYAQQHGK). Specific antibodies were affinity purified with the appropriate antigens.

Primary keratinocyte cultures

Keratinocytes isolated from embryos at E17.5 were cultured in PCT Epidermal Keratinocyte Medium (Chemicon). Differentiation was induced by adding $CaCl_2$ to a concentration of 1.2 mM, TGF-β to a concentration of 1 ng/ml (R&D) and LiCl to a concentration of 10 mM to the culture medium. BrdU was added to the medium (10 μM) and cells were incubated for 1 h before being fixed and processed for immunostaining. For growth curve analysis, 3×10^5 cells from passage 2 were plated in six-well plates, and the total numbers of cells were counted daily. Transfections were performed with Effectene reagents (Qiagen) or with polyethyleneimine (Sigma). Retroviral infections were performed according to standard protocols.

Immunoprecipitation, subcellular fractionation, western blot analysis and immunofluorescence

Primary keratinocytes were lysed in 25 mM Tris–HCl (pH 7.4), 150 mM NaCl, 1 mM EDTA, 1 mM $MgCl_2$, 0.2% Triton X-100, 0.3% NP-40, protease inhibitors and phosphatase inhibitors. Cell lysates were incubated for 2 h at 4°C with antibodies and then with protein A/G plus-agarose beads. Immunoprecipitates were subjected to western blot analysis. Separation of nuclear and cytoplasmic extracts was performed using NE-PER® Nuclear and Cytoplasmic Extraction Reagents (Pierce). Western blot analysis was performed using antibodies against YAP, p-YAP, MST1, p-MST1 (Cell Signaling), LATS1, LATS2 (Bethyl Laboratories Inc.), HA, filaggrin (Covance), laminin B (Santa Cruz), α-tubulin (Chemicon), Flag (Sigma) and WW45. For immunostaining analysis, keratinocytes were fixed and then exposed consecutively to primary and secondary antibodies. Slides were mounted with DAPI and imaged.

Supplementary data

Supplementary data are available at *The EMBO Journal* Online (http://www.embojournal.org).

Acknowledgements

We thank Dr H Saya for LATS1/2 cDNAs. This study was supported by grants from the NRL Program, the 21st Century Frontier Functional Human Genome Project, the Korea National Cancer Center Program and the Nuclear Research Grant.

References

Bennett FC, Harvey KF (2006) Fat cadherin modulates organ size in *Drosophila* via the Salvador/Warts/Hippo signaling pathway. *Curr Biol* **16:** 2101–2110

Blanpain C, Horsley V, Fuchs E (2007) Epithelial stem cells: turning over new leaves. *Cell* **128:** 445–458

Camargo FD, Gokhale S, Johnnidis JB, Fu D, Bell GW, Jaenisch R, Brummelkamp TR (2007) YAP1 increases organ size and expands undifferentiated progenitor cells. *Curr Biol* **17:** 2054–2060

Chan EH, Nousiainen M, Chalamalasetty RB, Schafer A, Nigg EA, Sillje HH (2005) The Ste20-like kinase Mst2 activates the human large tumor suppressor kinase Lats1. *Oncogene* **24:** 2076–2086

Chenn A, Walsh CA (2002) Regulation of cerebral cortical size by control of cell cycle exit in neural precursors. *Science* **297:** 365–369

Cho E, Feng Y, Rauskolb C, Maitra S, Fehon R, Irvine KD (2006) Delineation of a fat tumor suppressor pathway. *Nat Genet* **38:** 1142–1150

Dong J, Feldmann G, Huang J, Wu S, Zhang N, Comerford SA, Gayyed MF, Anders RA, Maitra A, Pan D (2007) Elucidation of a universal size-control mechanism in *Drosophila* and mammals. *Cell* **130:** 1120–1133

Edgar BA (2006) From cell structure to transcription: hippo forges a new path. *Cell* **124:** 267–273

Guo C, Tommasi S, Liu L, Yee JK, Dammann R, Pfeifer GP (2007) RASSF1A is part of a complex similar to the *Drosophila* Hippo/Salvador/Lats tumor-suppressor network. *Curr Biol* **17:** 700–705

Hamaratoglu F, Willecke M, Kango-Singh M, Nolo R, Hyun E, Tao C, Jafar-Nejad H, Halder G (2006) The tumour-suppressor genes NF2/Merlin and expanded act through Hippo signalling to regulate cell proliferation and apoptosis. *Nat Cell Biol* **8:** 27–36

Harvey K, Tapon N (2007) The salvador-warts-hippo pathway—an emerging tumour-suppressor network. *Nat Rev Cancer* **7:** 182–191

Harvey KF, Pfleger CM, Hariharan IK (2003) The *Drosophila* Mst ortholog, hippo, restricts growth and cell proliferation and promotes apoptosis. *Cell* **114:** 457–467

Hennings H, Michael D, Cheng C, Steinert P, Holbrook K, Yuspa SH (1980) Calcium regulation of growth and differentiation of mouse epidermal cells in culture. *Cell* **19:** 245–254

Hergovich A, Schmitz D, Hemmings BA (2006) The human tumour suppressor LATS1 is activated by human MOB1 at the membrane. *Biochem Biophys Res Commun* **345:** 50–58

Huang J, Wu S, Barrera J, Matthews K, Pan D (2005) The Hippo signaling pathway coordinately regulates cell proliferation and apoptosis by inactivating Yorkie, the *Drosophila* Homolog of YAP. *Cell* **122:** 421–434

Jia J, Zhang W, Wang B, Trinko R, Jiang J (2003) The *Drosophila* Ste20 family kinase dMST functions as a tumor suppressor by restricting cell proliferation and promoting apoptosis. *Genes Dev* **17:** 2514–2519

Jiang Z, Li X, Hu J, Zhou W, Jiang Y, Li G, Lu D (2006) Promoter hypermethylation-mediated down-regulation of LATS1 and LATS2 in human astrocytoma. *Neurosci Res* **56:** 450–458

Justice RW, Zilian O, Woods DF, Noll M, Bryant PJ (1995) The *Drosophila* tumor suppressor gene warts encodes a homolog of human myotonic dystrophy kinase and is required for the control of cell shape and proliferation. *Genes Dev* **9:** 534–546

Kango-Singh M, Nolo R, Tao C, Verstreken P, Hiesinger PR, Bellen HJ, Halder G (2002) Shar-pei mediates cell proliferation arrest during imaginal disc growth in *Drosophila*. *Development* **129:** 5719–5730

Lai ZC, Wei X, Shimizu T, Ramos E, Rohrbaugh M, Nikolaidis N, Ho LL, Li Y (2005) Control of cell proliferation and apoptosis by mob as tumor suppressor, mats. *Cell* **120:** 675–685

Lallemand D, Curto M, Saotome I, Giovannini M, McClatchey AI (2003) NF2 deficiency promotes tumorigenesis and metastasis by destabilizing adherens junctions. *Genes Dev* **17:** 1090–1100

Lee KK, Murakawa M, Nishida E, Tsubuki S, Kawashima S, Sakamaki K, Yonehara S (1998) Proteolytic activation of MST/Krs, STE20-related protein kinase, by caspase during apoptosis. *Oncogene* **16:** 3029–3037

Matallanas D, Romano D, Yee K, Meissl K, Kucerova L, Piazzolla D, Baccarini M, Vass JK, Kolch W, O'Neill E (2007) RASSF1A elicits apoptosis through an MST2 pathway directing proapoptotic transcription by the p73 tumor suppressor protein. *Mol Cell* **27:** 962–975

McClatchey AI, Giovannini M (2005) Membrane organization and tumorigenesis—the NF2 tumor suppressor, Merlin. *Genes Dev* **19:** 2265–2277

McClatchey AI, Saotome I, Ramesh V, Gusella JF, Jacks T (1997) The Nf2 tumor suppressor gene product is essential for extraembryonic development immediately prior to gastrulation. *Genes Dev* **11:** 1253–1265

McPherson JP, Tamblyn L, Elia A, Migon E, Shehabeldin A, Matysiak-Zablocki E, Lemmers B, Salmena L, Hakem A, Fish J, Kassam F, Squire J, Bruneau BG, Hande MP, Hakem R (2004) Lats2/Kpm is required for embryonic development, proliferation control and genomic integrity. *EMBO J* **23:** 3677–3688

Morin-Kensicki EM, Boone BN, Howell M, Stonebraker JR, Teed J, Alb JG, Magnuson TR, O'Neal W, Milgram SL (2006) Defects in yolk sac vasculogenesis, chorioallantoic fusion, and embryonic axis elongation in mice with targeted disruption of Yap65. *Mol Cell Biol* **26:** 77–87

Nolo R, Morrison CM, Tao C, Zhang X, Halder G (2006) The bantam microRNA is a target of the hippo tumor-suppressor pathway. *Curr Biol* **16:** 1895–1904

Okada T, Lopez-Lago M, Giancotti FG (2005) Merlin/NF-2 mediates contact inhibition of growth by suppressing recruitment of Rac to the plasma membrane. *J Cell Biol* **171:** 361–371

Olmeda D, Castel S, Vilaro S, Cano A (2003) Beta-catenin regulation during the cell cycle: implications in G2/M and apoptosis. *Mol Biol Cell* **14:** 2844–2860

Overholtzer M, Zhang J, Smolen GA, Muir B, Li W, Sgroi DC, Deng CX, Brugge JS, Haber DA (2006) Transforming properties of YAP, a candidate oncogene on the chromosome 11q22 amplicon. *Proc Natl Acad Sci USA* **103:** 12405–12410

Pan D (2007) Hippo signaling in organ size control. *Genes Dev* **21:** 886–897

Pantalacci S, Tapon N, Leopold P (2003) The Salvador partner Hippo promotes apoptosis and cell-cycle exit in *Drosophila*. *Nat Cell Biol* **5:** 921–927

Reya T, Morrison SJ, Clarke MF, Weissman IL (2001) Stem cells, cancer, and cancer stem cells. *Nature* **414:** 105–111

Saucedo LJ, Edgar BA (2007) Filling out the Hippo pathway. *Nat Rev Mol Cell Biol* **8:** 613–621

Schmahl W (1983) Developmental gradient of cell cycle in the telencephalic roof of the fetal NMRI-mouse. *Anat Embryol (Berl)* **167:** 355–364

Shipley GD, Pittelkow MR, Wille Jr JJ, Scott RE, Moses HL (1986) Reversible inhibition of normal human prokeratinocyte proliferation by type beta transforming growth factor-growth inhibitor in serum-free medium. *Cancer Res* **46:** 2068–2071

Silva E, Tsatskis Y, Gardano L, Tapon N, McNeill H (2006) The tumor-suppressor gene fat controls tissue growth upstream of expanded in the hippo signaling pathway. *Curr Biol* **16:** 2081–2089

St John MA, Tao W, Fei X, Fukumoto R, Carcangiu ML, Brownstein DG, Parlow AF, McGrath J, Xu T (1999) Mice deficient of Lats1 develop soft-tissue sarcomas, ovarian tumours and pituitary dysfunction. *Nat Genet* **21:** 182–186

Sudol M (1994) Yes-associated protein (YAP65) is a proline-rich phosphoprotein that binds to the SH3 domain of the Yes proto-oncogene product. *Oncogene* **9:** 2145–2152

Takahashi Y, Miyoshi Y, Takahata C, Irahara N, Taguchi T, Tamaki Y, Noguchi S (2005) Down-regulation of LATS1 and LATS2 mRNA expression by promoter hypermethylation and its association with biologically aggressive phenotype in human breast cancers. *Clin Cancer Res* **11:** 1380–1385

Tao W, Zhang S, Turenchalk GS, Stewart RA, St John MA, Chen W, Xu T (1999) Human homologue of the *Drosophila melanogaster* lats tumour suppressor modulates CDC2 activity. *Nat Genet* **21:** 177–181

Tapon N, Harvey KF, Bell DW, Wahrer DC, Schiripo TA, Haber DA, Hariharan IK (2002) salvador promotes both cell cycle exit and apoptosis in *Drosophila* and is mutated in human cancer cell lines. *Cell* **110:** 467–478

Thompson BJ, Cohen SM (2006) The Hippo pathway regulates the bantam microRNA to control cell proliferation and apoptosis in *Drosophila*. *Cell* **126:** 767–774

Udan RS, Kango-Singh M, Nolo R, Tao C, Halder G (2003) Hippo promotes proliferation arrest and apoptosis in the Salvador/Warts pathway. *Nat Cell Biol* **5:** 914–920

Vassilev A, Kaneko KJ, Shu H, Zhao Y, DePamphilis ML (2001) TEAD/TEF transcription factors utilize the activation domain of YAP65, a Src/Yes-associated protein localized in the cytoplasm. *Genes Dev* **15:** 1229–1241

Wei X, Shimizu T, Lai ZC (2007) Mob as tumor suppressor is activated by Hippo kinase for growth inhibition in *Drosophila*. *EMBO J* **26:** 1772–1781

Willecke M, Hamaratoglu F, Kango-Singh M, Udan R, Chen CL, Tao C, Zhang X, Halder G (2006) The fat cadherin acts through the hippo tumor-suppressor pathway to regulate tissue size. *Curr Biol* **16:** 2090–2100

Wu S, Huang J, Dong J, Pan D (2003) hippo encodes a Ste-20 family protein kinase that restricts cell proliferation and promotes apoptosis in conjunction with salvador and warts. *Cell* **114:** 445–456

Xia H, Qi H, Li Y, Pei J, Barton J, Blackstad M, Xu T, Tao W (2002) LATS1 tumor suppressor regulates G2/M transition and apoptosis. *Oncogene* **21:** 1233–1241

Xu T, Wang W, Zhang S, Stewart RA, Yu W (1995) Identifying tumor suppressors in genetic mosaics: the *Drosophila* lats gene encodes a putative protein kinase. *Development* **121:** 1053–1063

Yagi R, Chen LF, Shigesada K, Murakami Y, Ito Y (1999) A WW domain-containing yes-associated protein (YAP) is a novel transcriptional co-activator. *EMBO J* **18:** 2551–2562

Yang X, Yu K, Hao Y, Li DM, Stewart R, Insogna KL, Xu T (2004) LATS1 tumour suppressor affects cytokinesis by inhibiting LIMK1. *Nat Cell Biol* **6:** 609–617

Zender L, Spector MS, Xue W, Flemming P, Cordon-Cardo C, Silke J, Fan ST, Luk JM, Wigler M, Hannon GJ, Mu D, Lucito R, Powers S, Lowe SW (2006) Identification and validation of oncogenes in liver cancer using an integrative oncogenomic approach. *Cell* **125:** 1253–1267

Zhao B, Wei X, Li W, Udan RS, Yang Q, Kim J, Xie J, Ikenoue T, Yu J, Li L, Zheng P, Ye K, Chinnaiyan A, Halder G, Lai ZC, Guan KL (2007) Inactivation of YAP oncoprotein by the Hippo pathway is involved in cell contact inhibition and tissue growth control. *Genes Dev* **21:** 2747–2761

